

## Analog $E2$ transitions in the $A = 30$ nuclei; lifetime and branching ratio measurements of levels in $^{30}\text{P}$

A. Anttila and J. Keinonen

*Department of Physics, University of Helsinki, SF-00170 Helsinki 17, Finland*

(Received 11 May 1979)

The  $\gamma$ -ray decays of the first two  $J^\pi = 2^+$ ,  $T = 1$  states in  $^{30}\text{P}$  ( $T_z = 0$ ) at  $E_x = 2.938$  and  $4.183$  MeV have been studied through the  $^{29}\text{Si}(p,\gamma)^{30}\text{P}$  reaction. One new branch from the  $2.938$  MeV state and three new branches from the  $4.183$  MeV state were found. The recently reported isoscalar  $E2$  transition  $4.183(2^+,1) \rightarrow 0.677(0^+,1)$  MeV was confirmed and the relative intensity of  $(1.3 \pm 0.3)\%$  was determined. Employing the Doppler-shift attenuation (DSA) method, the lifetime  $\tau_m = (90 \pm 11)$  fs was determined for the  $2.938$  MeV state and in the present, exceptionally advantageous conditions the lifetime  $(3.1 \pm 0.9)$  fs for the  $4.183$  MeV state was determined for the first time. In the analysis, the Monte-Carlo method was employed. The  $E2$  branches  $2.938(2^+,1) \rightarrow 0.677(0^+,1)$  and  $4.183(2^+,1) \rightarrow 0.677(0^+,1)$  MeV are compared with the analog transitions in  $^{30}\text{Si}$  ( $T_z = +1$ ) and  $^{30}\text{S}$  ( $T_z = -1$ ) as well as with shell-model calculations.

NUCLEAR REACTION  $^{29}\text{Si}(p,\gamma)$ ,  $E = 0.73, 1.75$  MeV, measured  $\sigma(E;E_\gamma, \theta)$ , Doppler-shift attenuation.  $^{30}\text{P}$  levels, deduced  $\gamma$ -ray branching ratios,  $\tau_m$ . Implanted, enriched  $^{29}\text{Si}$  targets.

### I. INTRODUCTION

The first three members of the isospin  $T = 1$  triplet states have been identified in the  $A = 30$  nuclei  $^{30}\text{Si}$  ( $T_z = +1$ ),  $^{30}\text{P}$  ( $T_z = 0$ ), and  $^{30}\text{S}$  ( $T_z = -1$ ) [where the definition  $T_z = \frac{1}{2}(N - Z)$  is used], as shown, e.g., in Table 30.22 of Ref. 1 and in Fig. 1 of this paper. In the mirror nuclei  $^{30}\text{Si}$  and  $^{30}\text{S}$ , the analog states are the ground states and first and second excited states. Assuming isospin to be a good quantum number, the  $E2$  transition strengths [in Weisskopf units (W.u.)] for the transitions  $(2^+, 1)_1 \rightarrow (0^+, 1)_1$  and  $(2^+, 1)_2 \rightarrow (0^+, 1)_1$  can be expressed<sup>2</sup> in terms of two independent parameters, viz., isoscalar ( $S$ ) and isovector ( $V$ ) matrix elements:

$$|M(E2)|^2 = (S + T_z V)^2, \quad (1)$$

where the matrix elements have been reduced in space and isospace.

In the case of  $^{30}\text{Si}$ , the  $E2$  strengths are well established on the basis of several consistent experiments.<sup>1</sup> For  $^{30}\text{S}$  there is a large uncertainty in the  $E2$  strength of the  $2.211(2^+, 1)_1 \rightarrow 0(0^+, 1)_1$  MeV transition due to the scatter of lifetime values with a factor of 2; the value of  $(185 \pm 35)$  fs<sup>1</sup> has been adopted from the three values reported in the literature. The strength of the  $3.403(2^+, 1)_2 \rightarrow 0(0^+, 1)_1$  MeV transition is better known, the two values given in the literature being in agreement.<sup>1</sup> In  $^{30}\text{P}$  the strength values of the  $E2$  transition  $2.938(2^+, 1)_1 \rightarrow 0.677(0^+, 1)_1$  MeV reported in the literature range from  $|M(E2)|^2 = 8.9 \pm 1.6$  W.u. (Ref.

3) to 21 W.u. (Ref. 4); this is caused not only by the different results found for the lifetime of the  $2.938(2^+, 1)$  MeV state but partly also by the variety of branching ratios measured for the  $2.938(2^+, 1)_1 \rightarrow 0.677(0^+, 1)_1$  MeV transition. In the case of the  $4.183(2^+, 1)_2 \rightarrow 0.677(0^+, 1)_1$  MeV branch, which is obscured by the very strong  $M1$ ,  $\Delta T = 1$  transition  $4.183(2^+, 1) \rightarrow 0.709(1^+, 0)$  MeV, a recent search<sup>5</sup> yielded the intensity  $(2 \pm 1)\%$ . However, because only upper limits have been reported for the lifetime of the  $4.183$  MeV state, the adopted value being  $\tau_m < 20$  fs,<sup>1</sup> only the lower limit of  $0.20$  W.u. can be deduced for the important isoscalar  $E2$  strength.

In the present work, the experimental strength values of the isoscalar  $E2$  transitions  $2.938(2^+, 1)_1 \rightarrow 0.677(0^+, 1)_1$  and  $4.183(2^+, 1)_2 \rightarrow 0.677(0^+, 1)_1$  MeV were studied through the  $^{29}\text{Si}(p,\gamma)^{30}\text{P}$  reaction. The previously reported results are improved by utilizing a high performance Ge(Li) detector and by applying the methods developed in our laboratory (see, e.g., Ref. 6) for the determination of short nuclear lifetimes.

The experimental arrangements are described in Sec. II, while Sec. III presents the measurements and results. The  $E2$  strengths are discussed in Sec. IV in terms of shell-model calculations.

### II. EXPERIMENTAL ARRANGEMENTS

The  $2.5$  MV Van de Graaff accelerator at the University of Helsinki supplied the proton beam of about  $70 \mu\text{A}$ . The beam was collimated into a

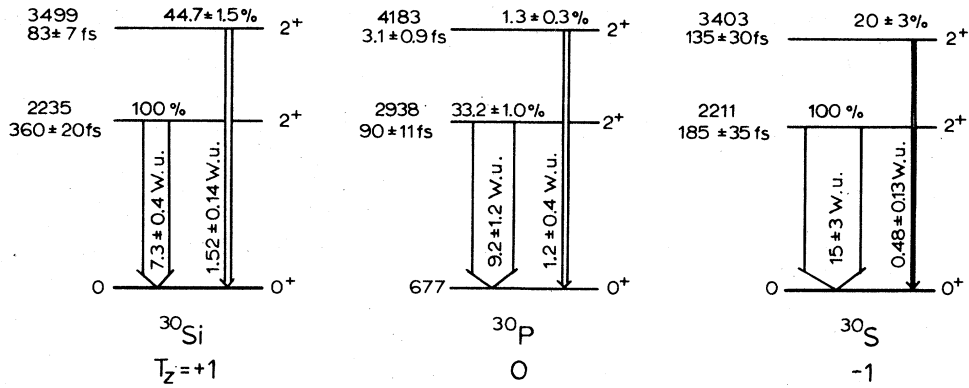


FIG. 1. Decay modes of the first two  $2^+$ ,  $T=1$  states to the first  $0^+$ ,  $T=1$  states in the  $A=30$  isobaric triplet. The experimental data in  $^{30}\text{Si}$  and  $^{30}\text{S}$  are taken from Ref. 1 and in  $^{30}\text{P}$  from the present work except for the  $E_x$  and  $J^\pi$  values (Ref. 1).

profile of 3 mm on the target. The  $^{29}\text{Si}$  targets, most suited for the Doppler-shift measurements, were prepared by implanting a  $4.4 \mu\text{g}/\text{cm}^2$  dose of 100 keV  $^{29}\text{Si}^+$  ions into 0.4 mm thick Ta backings in the isotope separator of the laboratory. The atomic ratios of  $^{29}\text{Si}$  to Ta were thus at maximum concentration being about 1 to 20. The  $\gamma$ -ray radiation was detected by a Princeton  $110 \text{ cm}^3$  Ge(Li) detector with an efficiency of 21.8%. The energy resolution of the detection system was 2.0 keV at  $E_\gamma=1.3 \text{ MeV}$  and 3.0 keV at  $E_\gamma=2.6 \text{ MeV}$ . The detector was mounted on a turntable centered on the beam spot on the target. Standard signal amplifying and analyzing equipment was used in conjunction with the detector. The stability of the spectrometer was checked with a  $^{208}\text{Tl}$   $\gamma$ -ray source.

### III. MEASUREMENTS AND RESULTS

#### A. Branching ratios

The  $\gamma$ -ray decay schemes of the  $E_x=2.938$  and 4.183 MeV states were studied with the  $^{29}\text{Si}(p, \gamma)^{30}\text{P}$  reaction at  $E_p=731 \text{ keV}$ . This resonance has been reported to have 80% decay to the 2.938 MeV state, 19% decay to the 4.183 MeV state, and only minor branches to the 1.454 MeV state (0.6%) and ground state (0.4%).<sup>4</sup>

The  $\gamma$ -ray spectra were recorded with the Ge(Li) detector at  $55^\circ$  with respect to the proton beam at a distance of 4 cm from the beam spot. The dispersion selected for the 4 K spectra was 1.81 keV/channel. The spectra with accumulated charges of 1 C were taken on the resonance and just below it. The efficiency of the detector was determined in the experimental geometry with revised  $\gamma$ -ray intensities in  $^{56}\text{Co}$  (Ref. 7) and using recently determined relative  $\gamma$ -ray intensities in the  $^{27}\text{Al}(p, \gamma)^{28}\text{Si}$  reaction at  $E_p=992 \text{ keV}$ .<sup>8</sup>

The  $\gamma$ -ray branching ratios obtained for the compound state at  $E_x=6.304 \text{ MeV}$  are given in Table I along with a comparison with previous values. In each case at least the stronger of the secondary transitions was observed, and the intensities corrected using the branching ratios from Ref. 1 were in agreement with those of the primary transitions. New transitions from the resonance state to the 1.973( $3^+$ ), 2.723( $2^+$ ), 2.839( $1^+$ ), and 3.019( $1^+$ ) MeV states were found.

The  $\gamma$ -ray branching ratios obtained for the 2.938 and 4.183 MeV states are summarized in Table II. In the case of the 2.938 MeV state a new transition to the 1.973( $3^+$ , 0) MeV state was found. In the case of the 4.183 MeV state, the transitions to the 1.454( $2^+$ , 0), 1.973( $3^+$ , 0), and 2.538( $3^+$ , 0) MeV states are reported for the first time. The interesting  $E2$  branch 4.183( $2^+$ , 1)  $\rightarrow$  0.677( $2^+$ , 1) MeV is illustrated in Fig. 2, where portions of the  $\gamma$ -ray spectra recorded in the Doppler-shift measurements are shown.

In order to obtain the correct  $E2$  transition strengths, the values given in Table II have been

TABLE I. Gamma decay scheme of the  $^{29}\text{Si}(p, \gamma)^{30}\text{P}$  reaction obtained at  $E_p=731 \text{ keV}$ , and comparison with the previous branchings.<sup>a</sup>

$E_f$ (MeV)	$J_f^\pi$	Relative intensity (%)	
		Present	Ref. 4
0	$1^+$	$1.1 \pm 0.3$	0.6
1.454	$2^+$	$0.7 \pm 0.3$	0.4
1.973	$3^+$	$0.8 \pm 0.3$	
2.723	$2^+$	$0.8 \pm 0.3$	
2.839	$1^+$	$0.6 \pm 0.3$	
2.938	$2^+, T=1$	$76.0 \pm 0.8$	80
3.019	$1^+$	$2.0 \pm 0.4$	
4.183	$2^+, T=1$	$18.0 \pm 0.6$	19

<sup>a</sup>The  $E_f$  and  $J_f^\pi$  values are taken from Ref. 1.

TABLE II. Gamma decay schemes of the  $2^+, T=1$  states at 2938 and 4183 keV in  $^{30}\text{P}$  and their comparison with the previous branchings.<sup>a</sup>

$E_i$ (MeV)	$J_i^\pi$	$E_f$ (MeV)	$J_f^\pi$	Relative intensity (%)	
				Present <sup>b</sup>	Previous
2.938	$2^+, T=1$	0	$1^+$	$16.4 \pm 0.8$	$17 \pm 2^c$
		0.677	$0^+, T=1$	$33.2 \pm 1.0$	$32 \pm 2^c$
		0.709	$1^+$	$5.4 \pm 0.6$	$9 \pm 2^c$
		1.454	$2^+$	$44.4 \pm 1.0$	$42 \pm 2^c$
		1.973	$3^+$	$0.6 \pm 0.2$	
4.183	$2^+, T=1$	0	$1^+$	$12.5 \pm 0.7$	$13 \pm 2^d$
		0.677	$0^+, T=1$	$1.3 \pm 0.3$	$2 \pm 1^d$
		0.709	$1^+$	$73.8 \pm 1.0$	$85 \pm 2^d$
		1.454	$2^+$	$4.4 \pm 0.9$	
		1.973	$3^+$	$3.8 \pm 0.3$	
		2.538	$3^+$	$4.2 \pm 0.3$	

<sup>a</sup>The  $E_x$  and  $J^\pi$  values are taken from Ref. 1.

<sup>b</sup>For inclusion of the angular distribution correction, see the text.

<sup>c</sup>Adopted value from Ref. 1.

<sup>d</sup>Reference 5.

corrected for the angular distributions. According to the angular distribution and correlation data given in Refs. 4 and 9, the  $P_4$  term has negligible contribution in the dominant  $M1$ ,  $\Delta T=1$  transitions

from the 2.938( $2^+, 1$ ) MeV state to the  $0(0^+, 0)$  and 1.454( $2^+, 0$ ) MeV states, and from the 4.183( $2^+, 1$ ) MeV state to the  $0(1^+, 0)$  and 0.709( $1^+, 0$ ) MeV states. Thus the solid angle integrated  $\gamma$ -ray in-

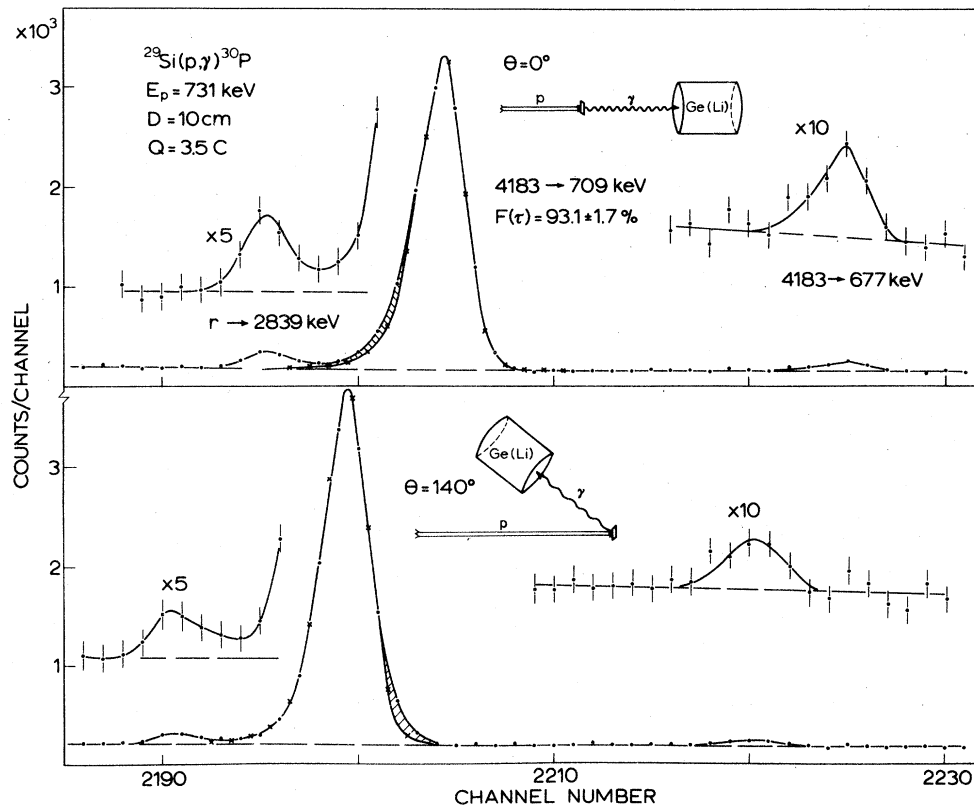


FIG. 2. Portions of  $\gamma$ -ray spectra recorded in the DSA measurements of the 3.474 MeV  $\gamma$  ray, 4.183  $\rightarrow$  0.709 MeV. The line shapes of photopeaks recorded at the angles  $0^\circ$  and  $140^\circ$  are taken from the photopeaks of the  $r \rightarrow 2.938$  MeV transition recorded at the same angles. In the insets the detector size and the target-detector distance are plotted on the same scale to illustrate the measuring geometry. The dispersion is 1.54 keV/channel.

tensity values are obtained at the angle of  $55^\circ$  relative to the beam. In the case of the weak M1 transitions, the  $P_4$  contribution is assumed to have negligible effect and is included in the error limits. Using the angular distribution data measured for the primary transitions  $\gamma - 2.938$  and  $\gamma - 4.183$  MeV,<sup>4,9</sup> the calculated angular distributions yield a 6% reduction to the observed intensity values of the E2 transitions  $2.938(2^+, 1) - 0.677(0^+, 1)$  and  $4.183(2^+, 1) - 0.677(0^+, 1)$  MeV. The correction factors  $Q_2$  and  $Q_4$  due to the finite detector were taken from Ref. 10.

### B. Lifetimes

The lifetimes of the 2.938 and 4.183 MeV states were studied in the present work with the Doppler-shift attenuation (DSA) method through the  $^{29}\text{Si}(p, \gamma)^{30}\text{P}$  reaction at  $E_p = 731$  keV. Owing to the extremely short lifetime of the 4.183 MeV state, the backing material must have high stopping power. For this reason tantalum backings with small  $^{29}\text{Si}$  doses (the atomic ratio of  $^{29}\text{Si}$  to Ta being about 1 to 20) were selected for the lifetime measurements. It should be emphasized that the uncertainty due to the implanted concentration in this case is insignificant compared to the advantages achieved. The measurements were performed with the Ge(Li) detector at angles of  $0^\circ$  and  $140^\circ$ . In order to reduce the geometric corrections due to the angular distributions of the  $\gamma$  rays, the target-detector distance of 10 cm was selected. The corrections for solid angle attenuation were taken into account using primary  $\gamma$  rays of the transitions  $\gamma - 2.938$  and  $\gamma - 4.183$  MeV. The experimental full shift was determined and used separately for each ( $0^\circ, 140^\circ$ ) sequence and the DSA measurements were repeated four times. The primary  $\gamma$  rays yielded an average value of  $(99.7 \pm 0.7)\%$  for the full shift, where the average is taken over all values. In this case, as in the lifetime measurements, photopeaks, single escape and double es-

cape peaks were used, when seen. The accumulated proton charge collected for each  $\gamma$ -ray spectrum was 3.5 C. The reason that no blistering or any other disturbing effect occurred in the Ta backed implanted target during the long proton bombardments is due to very high diffusion of hydrogen in Ta; the diffusion coefficient is of the order of  $10^{-6}$  and  $10^{-7}$   $\text{cm}^2/\text{s}$  at the temperatures of  $100^\circ$  and  $10^\circ\text{C}$  (Ref. 11), respectively. In order to have a confirmation of the DSA measurements, the  $E_p = 1746$  keV resonance<sup>4</sup> was also used to take identical measurements as for the case of the  $E_p = 731$  keV resonance.

A summary of the present lifetime measurements, the  $F(\tau)$  values with deduced mean lifetimes, is given in Table III. The DSA measurements of the 4.183 MeV state are illustrated in Fig. 2. As can be seen from the dashed areas, deduced by fitting the line shape of the full-shifted  $\gamma - 2.938$  MeV ( $E_\gamma = 3.366$  MeV) transition to that of the  $4.183 - 0.709$  MeV ( $E_\gamma = 3.474$  MeV) transition, the  $F(\tau)$  value is definitely less than 100%, i.e., attenuation of the  $4.183 - 0.709$  MeV transition occurs. In the fitting of the line shape the energy difference of 108 keV between the  $4.183 - 0.709$  and  $\gamma - 2.938$  MeV transitions was taken into account. Furthermore, according to measurements,<sup>4,9</sup> both transitions appear to have similar angular distributions, a fact which was also checked in the present work by the use of the intensity ratio for these transitions which was found to have the same value at each measuring angle.

The relevant data needed in the DSA analysis for description of the stopping of the recoiling  $^{30}\text{P}$  nuclei in Ta were taken from our earlier study,<sup>12</sup> where the experimental stopping parameters  $f_n = 0.67 \pm 0.08$  and  $f_e = 1.0 \pm 0.2$  were determined for  $^{27}\text{Al}$  recoiling in Ta, the stopping power being now given by

$$(d\epsilon/d\rho)_{\text{corr}} = f_n(d\epsilon/d\rho)_n^{\text{LSS}} + f_e(d\epsilon/d\rho)_e^{\text{LSS}}$$

TABLE III. Mean lifetimes observed for the  $2^+, T=1$  states at 2938 and 4183 keV in  $^{30}\text{P}$ .<sup>a</sup>

$E_x$ (keV)	$E_p$ (keV)	$E_\gamma$ (keV)	$F(\tau)$ (%)	$\tau_m$ (fs)	Present <sup>b</sup>	Previous <sup>c</sup>
2938	731	2261	31 $\pm$ 3	89 $\pm$ 12	90 $\pm$ 11	105 $\pm$ 20
		2938	28 $\pm$ 4	100 $\pm$ $\frac{26}{18}$		
	1746	2261	37 $\pm$ 2	92 $\pm$ 7		
4183	731	2938	39 $\pm$ 3	86 $\pm$ 9	3.1 $\pm$ 0.9	<20
		3474	93.1 $\pm$ 1.7	3.1 $\pm$ 0.7		
	1746	4183	91 $\pm$ 4	4 $\pm$ 2		
		3473	95.4 $\pm$ 2.1	2.8 $\pm$ 1.4		

<sup>a</sup>The  $E_p$  values are taken from Ref. 4 and  $E_x$  values from Ref. 1.

<sup>b</sup>The error limits quoted include the error limits of the experimental  $F(\tau)$  values and uncertainties due to the stopping process (see the text).

<sup>c</sup>Adopted value given in Ref. 1 (see the text).

TABLE IV. Experimental transition strengths of the 2.938 and 4.183 MeV states and their comparison with shell-model calculations.<sup>a</sup>

$E_i$ (MeV)	$E_f$ (MeV)	$J_i^{\pi}$	$J_f^{\pi}$	$T_m^b$ (fs)	Branching <sup>b</sup> (%)	$\delta^c$	M1 strengths ( $10^{-2}$ W.u.) theory				E2 strengths (W.u.) theory				
							expt. <sup>d</sup>	A	B	C	Ref. 20 <sup>e</sup>	Ref. 21 <sup>f</sup>	expt. <sup>d</sup>	D	E
2.938	0	$2^+, T=1$	$1^+$	$90 \pm 11$	$16.4 \pm 0.8$	$0.08 \pm 0.04$	$0.23 \pm 0.03$	4	1.3	5.3	$0.08 \pm 0.02$	$0.01 \pm 0.01$	0.1	0.0	$0.040 \pm 0.009$
	0.677		$0^+, T=1$			$1.9 \pm 0.3$	$0.50 \pm 0.014$					$0.96 \pm 0.14$			
	0.709		$1^+$			$33.2 \pm 1.0$	0 <sup>g</sup>					$9.2 \pm 1.2$	1.2	5.4	$8.9 \pm 2.6$
4.183	1.454		$2^+$		$5.4 \pm 0.6$	$0.03 \pm 0.03$	$0.17 \pm 0.03$	9.8	4.0	1.3	$0.41 \pm 0.09$	$1.6 \pm 0.3$	0.0	0.0	$0.010 \pm 0.002$
	0	$2^+, T=1$	$1^+$	$3.1 \pm 0.9$	$44.4 \pm 1.0$		$4.8 \pm 0.6$	73	22	14	62	$0.1 \pm 0.2$	0.1	0.1	$0.063 \pm 0.014$
	0.677		$0^+, T=1$		$12.5 \pm 0.7$	0 <sup>g</sup>	$1.8 \pm 0.5$	8.8	2.8	7.0	17	$4.6 \pm 1.4$	0.1	0.0	$0.17 \pm 0.08$
	0.709		$1^+$		$73.8 \pm 1.0$	$-0.01 \pm 0.08$	$18 \pm 5$	$9.8 \pm 0.9$	9.8	3.2	4.9	11	$0.01 \pm 0.11$	0.0	0.0
	1.454		$2^+$		$4.4 \pm 0.9$	$2.9 \pm 0.3$	$1.9 \pm 0.9$					60	$\pm 20$		
	1.973		$3^+$		$3.8 \pm 0.3$		$2.2 \pm 0.8$					14	$\pm 5$		
	2.538		$3^+$		$4.2 \pm 0.3$		$3.6 \pm 1.1$				24	$\pm 5$	34	$\pm 10$	
							10	$\pm 3$			24	$\pm 5$	170	$\pm 50$	

<sup>a</sup>The  $E_x$  and  $J^{\pi}$  values are taken from Ref. 1.<sup>b</sup>Present work.<sup>c</sup>Reference 4.<sup>d</sup>If the mixing ratios  $\delta(E2/M1)$  are not known, the values given are for pure transitions.<sup>e</sup>A: With bare-nucleon  $g$  factors. B: With the effective  $g$  factors  $g_p^e = 0.65 \pm 0.07$ ,  $g_n^e = -0.06 \pm 0.07$ ,  $g_{ps}^e = 4.02 \pm 0.15$ , and  $g_{ns}^e = -1.44 \pm 0.15$ . C: With effective single-particle matrix elements. D: With bare-nucleon charges. E: With the effective charges  $e_p + e_n = 2.12 \pm 0.08$  and  $e_p - e_n = 0.76 \pm 0.27$ .<sup>f</sup>With bare-nucleon  $g$  factors for M1 strengths and with effective charges  $e_p + e_n = 2.15$  and  $e_p - e_n = 1$  for E2 strengths. For error limits, see Ref. 21.<sup>g</sup>Only pure E2 transition is possible.

in the frame of the Lindhard, Scharff, Schiøtt (LSS) theory.<sup>13</sup> Our motive for this lies in the range measurements performed in our laboratory for the  $^{27}\text{Al} - \text{Ta}$  (Ref. 14) and  $^{34}\text{S} - \text{Ta}$  (Ref. 15) cases where the range values obtained for the 20–100 keV  $^{27}\text{Al}^+$  and  $^{34}\text{S}^+$  ions slowing down in Ta were found to have similar deviations from the LSS theory. In addition, since no abrupt changes have been observed in the earlier systematic studies on the ranges of light ions in Ta (Refs. 14 and 15), the previously obtained stopping parameters  $f_n = 0.67 \pm 0.15$  and  $f_e = 1.0 \pm 0.3$  with enlarged error limits due to the uncertainties of the interpolation, were adopted for the present  $^{30}\text{P} - \text{Ta}$  case. The results of Monte-Carlo calculations, which remove the  $\langle v \rangle \cos \varphi$  approximation,<sup>16</sup> and the experimental stopping parameter values were employed in the DSA analysis.

The present lifetime value of  $(90 \pm 11)$  fs obtained for the 2.938 MeV state is in good agreement with the lifetime  $(95 \pm 30)$  fs obtained in the recent  $^{27}\text{Al}(\alpha, n)^{30}\text{P}$  study.<sup>3</sup> The other values given in the literature are  $(35 \pm 5)$  fs (Ref. 4) and  $(70 \pm 10)$  fs (Ref. 17) from the  $(p, \gamma)$  reaction studies and  $(115 \pm 20)$  fs from a  $^{28}\text{Si}(\tau, p)^{30}\text{P}$  study (given as private communication in Ref. 1). The adopted value is taken to be  $(105 \pm 20)$  fs.<sup>1</sup> For the lifetime of the 4.183 MeV state only upper limits have been reported, these values being 20,<sup>3</sup> 40 (given as private communication in Ref. 1), 15,<sup>18</sup> 20,<sup>17</sup> and 24 fs,<sup>19</sup> and the adopted value is  $\tau_m < 20$  fs.<sup>1</sup>

#### IV. DISCUSSION

The experimental transition strengths of the 2.938 and 4.183 MeV states are given in Table IV along with the predictions of shell-model calculations. In the shell-model calculations by Glaudemans *et al.*<sup>20</sup> the  $M1$  strengths for  $^{30}\text{P}$  have been calculated using many-particle shell-model wave functions obtained from the best fit of the calculated energies to the experimental values in the mass region  $A=30-33$  and with bare-nucleon  $g$  factors (column A in Table IV), with the effective  $g$  factors obtained from a least-squares fit to experimental  $M1$  strengths in the  $A=30-32$  region (column B), and finally also with effective single-particle matrix elements from an analogous fit (column C). In the shell-model calculations by van Eijkern *et al.*<sup>21</sup> the  $M1$  strengths were calculated employing wave functions obtained with a similar fixing procedure in the  $A=28-32$  region and with bare-nucleon  $g$  factors. If we exclude the strong 4.183–0.709 MeV transition, where the strengths calculated with bare-nucleon  $g$  factors are in fair agreement with the experimental value, the  $M1$  transition strengths are strongly overestimated by these calculations.

In the case of  $E2$  transitions, Glaudemans *et al.*<sup>20</sup> used a similar technique as for  $M1$  transitions to obtain effective charges by fitting experimental  $E2$  data (columns D and E). The  $E2$  strengths 5.4 and 0.8 W.u. (Ref. 20) obtained for the transitions  $2.938(2^+, 1) - 0.677(0^+, 1)$  MeV and  $4.183(2^+, 1) - 0.677(0^+, 1)$  MeV with the effective proton charge  $e_p = 1.44 e$  and neutron charge  $e_n = 0.68 e$  are not in disagreement with the present experimental values of  $(9.2 \pm 1.2)$  and  $1.2 \pm 0.4$  W.u., respectively. The calculations by van Eijkern *et al.*<sup>21</sup> reproduce, with the effective charges  $e_p = 1.575 e$  and  $e_n = 0.575 e$ , the  $E2$  strengths  $(8.9 \pm 2.6)$  W.u. for the  $2.938(2^+, 1) - 0.677(0^+, 1)$  MeV transition, in fair agreement with the present experimental value. However, no branching is predicted for the  $4.183(2^+, 1) - 0.677(0^+, 1)$  MeV transition.

According to Eq. (1), where the isospin was assumed to be a good quantum number, the square roots of the experimental  $E2$  strengths in the  $A=30$  isobaric triplet (Fig. 1) plotted as a function of  $T_z$  should lie on a straight line. In Fig. 3 the solid lines illustrate the linear isospin dependences of the  $E2$  transition matrix elements in the transitions  $(2^+, 1)_1 - (0^+, 1)_1$  and  $(2^+, 1)_2 - (0^+, 1)_1$ . With the least-squares fit to the  $(2^+, 1)_2 - (0^+, 1)_1$  data, the linear isospin dependence is verified with the values  $S^2 = (0.94 \pm 0.11)$  W.u. and  $V^2 = (0.07 \pm 0.04)$  W.u. for  $\chi^2 = 0.4$ . In the case of the  $(2^+, 1)_1 - (0^+, 1)_1$  transitions, where the lifetime values reported in the literature for  $^{30}\text{S}$  (Ref. 1) have a large scatter, the isospin dependence is illustrated with the solid line plotted through the accurate  $^{30}\text{Si}$  and  $^{30}\text{P}$  values only. The linearity is now described by the values  $S^2 = (9.2 \pm 0.8)$  W.u. and  $V^2 = (0.11 \pm 0.08)$  W.u. In

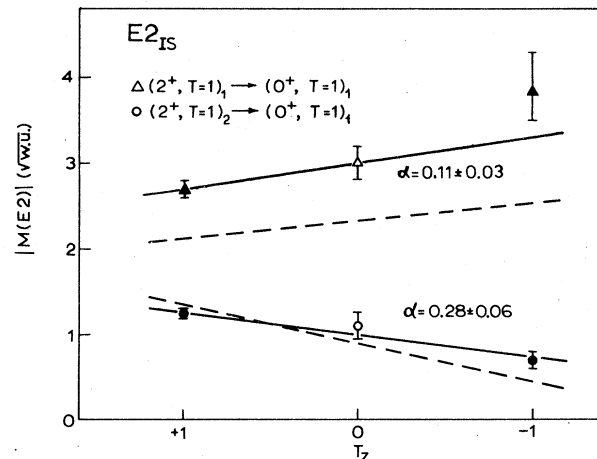


FIG. 3. The square roots of the  $E2$  transition strengths plotted as a function of  $T_z$ . The solid lines illustrate the fits to the experimental data (see the text) and the dashed lines the values obtained from a shell-model calculation (Ref. 20).

both cases the isoscalar and isovector strengths show a strong enhancement of the isoscalar  $E2$  strengths.

By writing the reduced single-particle matrix elements for an  $E2$  transition in terms of effective proton and neutron charge  $e_p$  and  $e_n$ ,<sup>20</sup> respectively, i.e., the  $E2$  strength in the form

$$|M(E2)|_{w.u.}^2 = [\delta_{T_i T_f} \beta_s (e_p + e_n) - \langle T_i T_{zi} 10 | T_f T_{zf} \rangle \beta_v (e_p - e_n)]^2, \quad (2)$$

the ratio  $\alpha$  of the isovector part to the isoscalar part can be written as

$$\alpha = \left(\frac{3}{2}\right)^{1/2} \frac{e_p - e_n}{e_p + e_n}, \quad (3)$$

where the coefficient  $1/\sqrt{2}$  is the Clebsch-Gordan coefficient  $\langle 1010 | 00 \rangle$  and  $\sqrt{3}$  arises from the ratio  $\beta_v/\beta_s$  of the charge independence parts of the reduced single-particle matrix elements as given in

the Appendix of Ref. 20. The experimental values of  $\alpha$  in the  $A=30$  isobaric triplet are  $0.11 \pm 0.03$  and  $0.28 \pm 0.06$  for the transitions  $(2^+, 1)_1 \rightarrow (0^+, 1)_1$  and  $(2^+, 1)_2 \rightarrow (0^+, 1)_1$ , respectively, whereas with the effective charges used in Refs. 20 and 21 the values are  $\alpha = 0.44$  and  $0.57$ , respectively. The current smaller values of  $\alpha$  suggest that the difference between the effective proton and neutron charges is smaller than obtained in the calculations.<sup>20,21</sup> As pointed out in Ref. 2, the additional isovector charge  $[(e_p - e_n)/e] - 1$  arises from  $T=1$  core excitations and the additional isoscalar charge  $[(e_p + e_n)/e] - 1$  from  $T=0$  core excitations. Thus the present results indicate the existence of appreciably higher  $T=1$ ,  $E2$  transition strengths arising from polarization of the  $^{28}\text{Si}$  core than predicted in the shell-model calculations, and further, in the cases of the  $(2^+, 1)_1 \rightarrow (0^+, 1)_1$  transitions, stronger core polarization than in the  $(2^+, 1)_2 \rightarrow (0^+, 1)_1$  transitions, where the initial states lie at about 1.2 MeV higher excitation energies.

<sup>1</sup>P. M. Endt and C. van der Leun, Nucl. Phys. **A310**, 1 (1978).

<sup>2</sup>E. K. Warburton and J. Weneser, in *Isospin in Nuclear Physics*, edited by D. H. Wilkinson (North-Holland, Amsterdam, 1969), Chap. 5.

<sup>3</sup>J. F. Sharpey-Schafer, P. R. Alderson, D. C. Bailey, J. L. Durell, W. M. Greene, and A. N. James, Nucl. Phys. **A167**, 602 (1971).

<sup>4</sup>G. I. Harris, A. K. Hyder, and J. Walinga, Phys. Rev. **187**, 1413 (1969).

<sup>5</sup>E. Kuhlmann and S. S. Hanna, Phys. Rev. C **10**, 1593 (1974).

<sup>6</sup>M. Bister, A. Anttila, and J. Keinonen, Phys. Rev. C **16**, 1303 (1977).

<sup>7</sup>M. Hautala, A. Anttila, and J. Keinonen, Nucl. Instrum. **150**, 599 (1978).

<sup>8</sup>A. Anttila, J. Keinonen, M. Hautala, and I. Forsblom, Nucl. Instrum. **147**, 501 (1977).

<sup>9</sup>E. E. Boart, L. L. Green, and J. C. Willmott, Proc. Soc. London **79**, 237 (1962).

<sup>10</sup>D. C. Camp and A. L. van Lehn, Nucl. Instrum. **76**, 192 (1969).

<sup>11</sup>J. Vöckl and G. A. Kefeld, in *Diffusion in Solids*, edited

by A. S. Novick and J. J. Burton (Academic, New York, 1975), p. 231.

<sup>12</sup>M. Bister, A. Anttila, and J. Keinonen, Phys. Lett. **53A**, 471 (1975).

<sup>13</sup>J. Lindhard, M. Scharff, and N. E. Schiøtt, K. Dan. Vidensk. Selsk. Mat. Fys. Medd. **33**, No. 14 (1963).

<sup>14</sup>A. Anttila, M. Bister, A. Fontell, and B. Winterbon, Radiat. Eff. **33**, 13 (1977).

<sup>15</sup>J. Keinonen, M. Hautala, M. Luomajärvi, A. Anttila, and M. Bister, Radiat. Eff. **39**, 189 (1978).

<sup>16</sup>A. E. Blaugrund, Nucl. Phys. **88**, 501 (1966).

<sup>17</sup>M. Bini, P. G. Bizzetti, A. M. Bizzetti-Sona, A. Cambi, M. Mando, and P. R. Maurenzig, Nuovo Cimento **4A**, 45 (1971).

<sup>18</sup>A. Lechaine and B. Hiral, Can. J. Phys. **48**, 2336 (1970).

<sup>19</sup>R. Graves and D. K. McDaniels, Bull. Amer. Phys. Soc. **14**, 1173 (1969).

<sup>20</sup>P. W. M. Glaudemans, P. M. Endt, and A. E. L. Dieperink, Ann. Phys. (N.Y.) **63**, 134 (1971).

<sup>21</sup>F. E. H. van Eijkern, G. A. Timmer, F. Meurders, and P. W. M. Glaudemans, Z. Phys. **A278**, 337 (1976).